Type of the Paper - Article

Soil Moisture in the Biebrza Wetlands Retrieved from Sentinel-1 Imagery

Katarzyna Dabrowska–Zielinska[1,*], Jan Musial[1], Alicja Malinska[1], Maria Budzynska[1], Radosław Gurdak[2], Wojciech Kiryla[1], Maciej Bartold[2], Patryk Grzybowski[1]

[1] Institute of Geodesy and Cartography, Jacka Kaczmarskiego 27, 02-679 Warsaw, Poland;
[2] University of Warsaw, Faculty of Geography and Regional Studies, Department of Geoinformatics, Cartography and Remote Sensing, Krakowskie Przedmiescie 30, 00-927 Warsaw, Poland;
* Correspondence: katarzyna.dabrowska-zielinska@igik.edu.pl; Tel.: +48-22-3291974

Abstract:

Soil moisture (SM) plays an essential role in environmental studies related to wetlands, an ecosystem sensitive to climate change. Hence, there is the need for its constant monitoring. SAR (Synthetic Aperture Radar) satellite imagery is the only mean to fulfill this objective regardless of the weather. The objective of the study was to develop the methodology for SM retrieval under wetland vegetation using Sentinel-1 (S-1) satellite data. The study was carried out during the years 2015–2017 in the Biebrza Wetlands, situated in northeastern Poland. At the Biebrza Wetlands, two Sentinel-1 validation sites were established, covering grassland and marshland biomes, where a network of 18 stations for soil moisture measurement was deployed. The sites were funded by the European Space Agency (ESA), and the collected measurements are available through the International Soil Moisture Network (ISMN). The NDVI (Normalized Difference Vegetation Index) was derived from the optical imagery of a MODIS (Moderate Resolution Imaging Spectroradiometer) sensor onboard the Terra satellite. The SAR data of the Sentinel-1 satellite with VH (vertical transmit and horizontal receive) and VV (vertical transmit and vertical receive) polarization were applied to soil moisture retrieval for a broad range of NDVI values and soil moisture conditions. The new methodology is based on research into the effect of vegetation on backscatter (σ°) changes under different soil moisture and vegetation (NDVI) conditions. It was found that the state of the vegetation may be described by the difference between σ° VH and σ° VV, or the ratio of σ° VV/VH, as calculated from the Sentinel-1 images. The most significant correlation coefficient for soil moisture was found for data that was acquired from the ascending tracks of the Sentinel-1 satellite, characterized by the lowest incidence angle, and SM at a depth of 5 cm.

The study demonstrated that the use of the inversion approach, which was applied to the new developed models and includes the derived indices based on S-1, allowed the estimation of SM for peatlands with reasonable accuracy (RMSE ~ 10 vol. %). Due to the temporal frequency of the two S-1 satellites' (S-1A and S-1B) acquisitions, it is possible to monitor SM changes every six days. The conclusion drawn from the study emphasizes a demand for the derivation of specific soil moisture retrieval algorithms that are suited for wetland ecosystems, where soil moisture is several times higher than in agricultural areas.

Keywords: Sentinel-1 backscatter; polarization; Terra MODIS; NDVI; soil moisture

1. Introduction

The soil moisture (SM) is an essential variable in environmental studies related to wetlands as it controls the biophysical processes that influence water, energy, and carbon exchanges. Hence, there is the need for SM constant monitoring. The SAR satellite imagery is the only mean to fulfill this objective regardless of cloud cover and, especially in the areas, in which deployment of in-situ SM measurements is not possible or economically unprofitable. The possibility of using high temporal and spatial resolution of the Sentinel-1 (S-1) imagery motivated authors to develop the methodology

for its retrieval based on backscattering coefficient (σ°), as calculated from the VH and VV polarizations.

The study was conducted in the Biebrza Wetlands, situated in northeastern Poland, with a total area of 59,233 ha. The wetlands are unique in Europe for their non-drained floodplains, marshes, and fens, surrounded by a post-glacial landscape. The Biebrza Wetlands holds 25,494 ha of peatlands, much biodiversity in the rich plant habitats, as well as highly diversified fauna, especially for birds [1]. This is still one of the wildest areas in Europe, and one of the areas that has been least destroyed, damaged, or changed by human activity. The Biebrza Wetlands were designated as a wetland site of global importance, as part of NATURA 2000, and since 1995 it has been under the protection of the RAMSAR Convention. Changes in soil moisture towards moisture depletion cause changes in the soil, and the release of substantial amounts of carbon into the atmosphere [2, 3]. Therefore, monitoring of soil moisture is very important for the management of the wetlands, to prevent peat degradation. The retrieval of soil moisture (SM) estimates by the means of satellite data is of great interest for a wide range of hydrological applications. The demand for operational SM monitoring was raised in numerous studies, and this was emphasized by the Global Climate Observing System (GCOS) by endorsing SM as an Essential Climate Variable (ECV).

Wetlands are often areas of limited access, where field sampling is difficult due to the inaccessible terrain and the seasonally dynamic nature of the area, and therefore satellites can provide information on the types of wetland vegetation and the dynamics of the local water cycle, in which soil moisture is a significant factor. Controlling soil moisture content is essential for the protection of peat-forming plant communities and for slowing down the drying processes against mineralization [4].

There are numerous studies that describe different techniques for monitoring the soil moisture of the wetlands area, however the SAR data give very good possibility for frequent spatial monitoring. The advances in soil moisture retrieval applying SAR data described Kornleson and Coulibaly [5]. The researchers have proved that microwave backscatter (σ°) is affected by the moisture and roughness of the canopy-soil layer. It is further affected by satellite sensor configurations such as the incident angle and the electromagnetic wave polarization [6, 7]. The strong interactions of the backscatter signal with the soil and vegetation may not be expressible by using simple linear functions. Atema and Ulaby [8], and Dabrowska et al. [9] proposed a water cloud model that characterized vegetation as the cloud that represented the total backscatter from the canopy as the sum of the contribution of the vegetation σ°_{veg}, and of the underlying soil σ°_{soil}. The separation of vegetation that is influenced by the soil moisture by the received microwave signals is not straightforward. The signal strongly depends on the type of vegetation, the amount of moisture, and the type of ecosystem [9]. Wetlands are characterized by deep peat layers, and it is not possible to compare agriculture ecosystems to wetlands, which are wet and very different. Thus, the models derived for wetlands have to be treated separately from models that are designated for agriculture soils and agriculture vegetation.

The C-band SAR on board the ERS-1/2 (European Remote Sensing) satellite, also on board the ENVISAT (ENVIronmental SATellite) satellite, and following the Sentinel-1 satellite, has been applied for soil moisture retrieval [5, 10]. The researchers used different models to distinguish the influence of vegetation and soil moisture on the microwave signal. Most of the methods that are applied for soil moisture retrieval have been developed for bare soils and agricultural areas [5, 11, 12, 13, 14, 15], and only a few have been found for natural environments such as wetlands. Mattia et al. [16] and Balenzano et al. [17] present the SMOSAR (Soil MOisture) algorithm for soil moisture retrieval using the multi-temporal SAR data from Sentinel-1. Paloscia et al. [18] developed soil moisture content (SMC) algorithm for Sentinel-1 characteristics, based on an artificial neural network (ANN), which was tested and validated in several test areas in Italy, Australia, and Spain. Also, ANN-based algorithms for the SMC retrieval applying C-band SAR data (ENVISAT/ASAR, Cosmo-SkyMed) have been adapted and presented by Santi et al. [19]. The overview of the retrieval algorithms presented in [19] demonstrated that ANN is a very powerful tool for estimating the soil moisture at both local and global scales. The proposed model simulates the backscatter of the

vegetated areas as a function of the soil backscatter, and the vegetation water content as computed from the NDVI. Kasischke et al. [20] conducted an investigation on the response of the ERS C-band SAR backscatter to variations in soil moisture and surface inundation in Alaskan wetlands, and found a positive correlation between the backscatter and soil moisture in sites that were dominated by herbaceous vegetation cover. Multi-temporal C-band SAR data, HH (horizontal transmit and horizontal receive), and VV polarized from ERS-2 and ENVISAT satellites were used by Lang et al. [21] for the investigation of inundations and soil moisture determination at wetlands. Santi et al. [22] carried out an investigation in an agricultural area located in North-west Italy, and found that the soil moisture values retrieved from the C-band ENVISAT/ASAR simulated by a hydrological model, and the measured values in situ, were in good agreement. Dabrowska-Zielinska et al. [23] conducted an investigation on soil moisture monitoring in the Biebrza Wetlands using Sentinel-1 data. There are not many studies for wetlands SM retrieval applying S-1 data, as can be seen from the literature review. Most of the publications refer to agriculture crops. Vreugdenhil et al. [24] examined the sensitivity of Sentinel-1 to vegetation dynamics and examined VV and VH backscatter and their ratio VH/VV to monitor crop conditions with special reference to vegetation water content (VWC) of agriculture crop. Greifeneder et al. [25] also analyzed the added value of the ratio of VH/VV for soil moisture estimates and demonstrated that the ratio of VH/VV allows a good compensation of vegetation dynamics for the retrieval of soil moisture.

The aim of this research study was to examine the sensitivity of Sentinel-1 backscatter (σ°) to SM variation under vegetation, as characterized by different biomasses, and to develop the new models for SM retrieval under wetland vegetation cover, by applying the C-band SAR data VH and VV polarized, which are available from the Sentinel-1 (S-1) satellite. The vegetation biomass was represented by NDVI, which was calculated by applying the Terra MODIS data. It was found that the indices, such as the difference of σ° (VH−VV) and the ratio of σ° VV/VH, are in monotonic relationships with NDVI. This will give quick information on the soil moisture, using only the Sentinel-1 data. In the developed model, the VV/VH ratio was used as the attenuation factor describing the level of ground and vegetation canopy interaction. The authors used the statistical approach to retrieve soil moisture at grassland and marshland sites taking the time series measurements of in-situ and satellite data. The most significant correlation between backscatter and soil moisture was found for the ascending tracks of Sentinel-1, and for a 5 cm depth of soil moisture.

The authors are motivated to undertake this study due to the lack of operational methods for the monitoring of SM based on Sentinel-1 data in the Central European wetlands areas. The presented study is a new approach to the previous one [23] on SM modelling based on S-1 data. Due to the temporal frequency of the two S-1 satellites' (S-1A and S-1B) acquisitions, it is possible to monitor soil moisture changes every six days with high spatial resolution (10x10 m). The results will highlight the contribution of S-1 data in soil moisture assessment, improving hydrological studies carried out in wetlands, which have so far been based on in–situ observations.

2. Materials and Methods

2.1. Study Area

The Biebrza Wetlands belong to the largest of Poland's National Parks—Biebrza National Park (BNP), which was created on September 9, 1993 [26]. It is located in Podlaskie Voivodeship, northeastern Poland, and it is situated along the Biebrza River. The geographical position of the study area is: UL: N54° E22°10' and LR: N53°10' E23°30'. The Biebrza Wetland area is flat with an average altitude of about 105 m above sea level (a.s.l.). To the north, the altitude increases, reaching approximately 120 m a.s.l. The main river is the Biebrza River, which flows out near the eastern border of Poland. The Biebrza River drainage basin area is 7051 km^2, the river length is 155 km, and its mean flow is 35.3 m^{3}s^{-1}. The Wetlands are flooded annually in the spring, and besides precipitation, flooding is the main supply of moisture into the peat soil. The weather in the Biebrza River Valley is one of the coolest in Poland—the mean year daily temperature is 6.5 °C. The mean sum of the yearly

precipitation ranges between 550–650 mm, and is one of the lowest in Poland. The length of the growing season is less than 200 days, and this is one of the shortest in Poland. Generally, summer is warm but short; winter is cold and long. The coldest month is January, with a mean temperature of -4.2 °C, and with temperatures dropping as low as −50 °C. Snow cover can last up to 140 days. July is the warmest month in the Biebrza Valley, with mean temperatures of 17.5 °C, and with temperatures increasing up to 35.3 °C. The length of the summer ranges between 77–85 days [27].

At the Biebrza Wetlands, two sites for Sentinel-1 (S-1) soil moisture (SM) retrieval were established (grassland and marshland), where a network of soil moisture ground stations was built (Fig. 1).

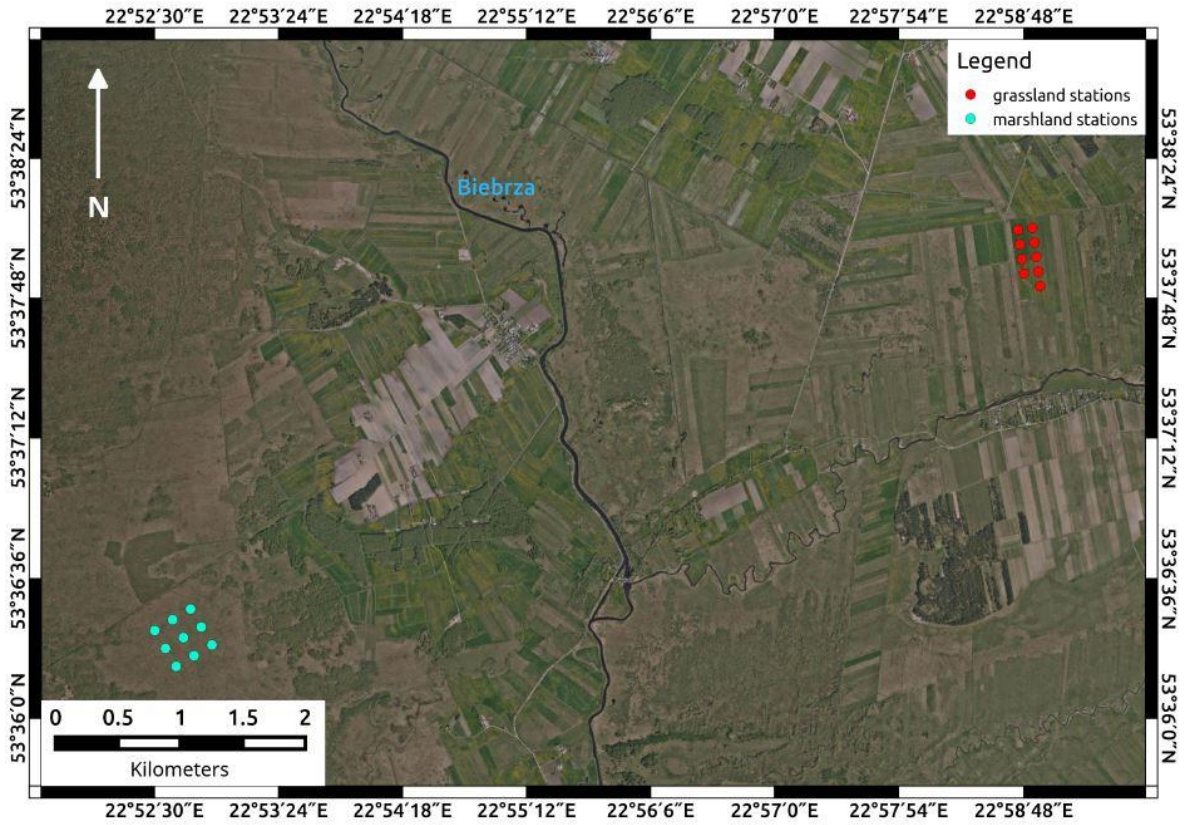

Figure 1. Location of S-1 soil moisture sites at the Biebrza Welands overlapped to the Geoportal maps image (www.geoportal.gov.pl).

Both sites had a flat topography and homogeneous land cover, which ensured the representativeness of average SM estimates across the sites. The environmental conditions between both sites varied with respect to the SM level, vegetation density, and the type of vegetation community cover. The soil moisture for these two sites differed. For the same years, the SM median for the grassland site was equal to 35 vol. % and it was much higher for the marshlands—close to 60 vol. %. The grassland site (Fig. 2) was located on an intensively mowed, drained meadow with semi–organic soil (muck-peat soil). The marshland site (Fig. 3) was located within the Biebrza National Park, and covered unmanaged sedges with more moist organic soil (peat soil).

Peer-reviewed version available at Remote Sens. 2018, 10, 1979; doi:10.3390/rs10121979

Figure 2. Grassland site.

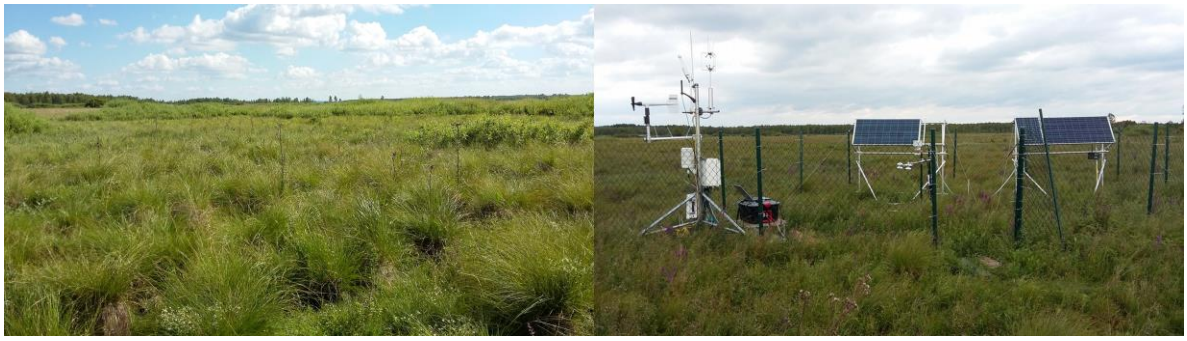

Figure 3. Marshland site.

The marshland site had a regular 500 × 500 m measuring grid composed of nine SM stations equipped with five probes each, measuring at the following depths: 5, 10, 20, and 50 cm. The grassland site had analogous instrumentation, with the stations arranged in two rows (230 × 580 m), one with four SM stations, and the second with five SM stations. In total, 90 Decagons GS3 soil moisture sensors were installed.

The grassland and marshland sites featured different soil moisture values and both sites were flooded during the spring. At the marshland site, the water table was very high; therefore, only the soil layer at 5 cm exhibited noticeable variations in water content. The deeper layers were close to saturation point (80–90 vol. %) through the year. An apparent drop of SM values that occurred in winter was related to the ground freezing. At the grassland site, the water table was lower; thus, only the 50 cm soil layer was permanently close to saturation level. The surface soil layers featured a strong annual cycle with a maximum amplitude of around 60 vol. %. A more in-depth description of the sites is available in [28]. The measurements collected from both sites are available through the International Soil Moisture Network (ISMN) [29].

2.2. In Situ Data

The in situ data were collected during field campaigns carried out in the years 2015–2017, simultaneous to the satellite overpasses. The positions of the measurement plots were determined using GPS (Global Positioning System). This information was essential for preparing the layer of special measurement points that was needed for the reading and processing of satellite data. Soil moisture (volumetric in %) was measured by 90 Decagons GS3 sensors calibrated to specific soil conditions at four depths: 5, 10, 20, and 50 cm. The GS3 sensor uses an electromagnetic field to measure the dielectric permittivity of the surrounding medium. The dielectric value is then converted to substrate water content by a calibration equation that is specific to the soil condition. Regarding the observation modes, the SM measurements were performed every 15 minutes. Additionally, the

height of the vegetation (m) and the biomass wet and dry (gm^{-2}) were measured. These data supported the SM analysis with ancillary information about the variables influencing the SAR signal (biomass, vegetation condition).

During the course of the study, the season of 2015 was extremely dry, whereas conditions in 2017 were extremely wet. In 2016, soil moisture levels were regarded as being average.

2.3. Satellite Data

Within the study, the following satellite images were used: Sentinel-1 and Terra MODIS. From the SciHUB (Sentinel Scientific Data Hub), Sentinel-1 Level-1 GRDH (Ground Range Detected at High resolution) products, in IWS (Interferometric Wide Swath) acquisition mode (spatial resolution 10 × 10 m) and in a WGS84 ellipsoid, were downloaded. The S-1 images were acquired in the C-band (5.5 GHz) in dual polarization: VV and VH. The nominal acquisition frequency of a single S-1 satellite over the Biebrza Wetlands during the period of the study was 12 days for a single track. However, the grassland site was covered by four different S-1 tracks (two descending and two ascending orbits), and the marshland site was covered by three different S-1 tracks (one descending and two ascending orbits). Furthermore, the availability of the two Sentinel-1A and Sentinel-1B platforms doubled the revisit time, which on average equaled four days for a single satellite and two–three days for two satellites. Table 1 presents the tracks and local incidence angles at the grassland and marshland test sites for selected S-1 relative orbits.

Table 1. Local incidence angles for selected S-1 orbit passes (A-ascending, D-descending) and tracks.

Pass/Track	Marshland incidence angle	Grassland incidence angle
A/29	43.49°	43.10°
A/131	35.59°	35.13°
D/80	-	45.65°
D/153	38.57°	38.18°

MODIS images as MOD09Q1 version 6 (V006) products were downloaded from the US Geological Survey website. The MOD09Q1 V006 product provided Bands 1 and 2 (620–670, 841–876, appropriately) at a 250 m resolution in an 8 day gridded level-3 product in the sinusoidal projection. The surface spectral reflectances of Bands 1–2 were corrected for atmospheric conditions such as gasses, aerosols, and Rayleigh scattering. For each pixel, a value was selected from all of the acquisitions within the 8-day composite period, taking into account the cloud coverage and the solar zenith angle [30].

The pass times of Sentinel-1 and Terra MODIS (8-day compositions) were close to each other; therefore, it was assumed that NDVI values could be used to represent the vegetation effect for the modeling of the backscattering coefficients of the S-1. MODIS 8-day data was smoothed to a one-day time series, and the data was synchronized with the Sentinel-1 date of acquisition. The area of an SM sensor is 500 × 500 m. This was taken as the average of the σ° S-1 values from 50 × 50 pixels for this area, and the average of the NDVI values from MODIS, from 2 × 2 pixels.

2.4. Methods

Sentinel-1 products were processed with the Sentinel-1 Toolbox (SNAP S1TBX v5.0.4 software) software provided by the European Space Agency (ESA). The processing included: speckle filtering applying a Lee Sigma speckle filter, radiometric calibration, and data conversion to a backscattering coefficient (σ°) (dB). Then, the scenes were geometrically registered to the local projection PUWG1992, and the σ° S-1 values, which corresponded to the measurement points, were extracted (5 × 5 pixels) using ERDAS software (Hexagon Geospatial/Intergraph®, Norcross, GA, USA).

Peer-reviewed version available at Remote Sens. 2018, 10, 1979; doi:10.3390/rs10121979

The methodology consists of models that were developed for soil moisture retrieval by applying the following Sentinel-1 data: VH and VV polarizations, VH-VV, VV/VH and the NDVI values from the Terra MODIS data.

2.4.1. Vegetation Descriptors

First, it was assumed that the vegetation index (NDVI) derived from Terra MODIS (described in section 2.3) could be used as a proxy for the vegetation descriptor of biomass.

Second, the vegetation biomass (expressed by NDVI) was represented by two combinations of sigma VH and sigma VV—the difference and the ratio. This assumption was performed following the approach of using the sigma difference VH–HH as the roughness of the vegetation (in this case, NDVI) following Rao et al. [31]. The σ° VH and σ° VV values were taken from the processed Sentinel-1 data (described in section 2.3).

The popular NDVI index works as an indicator that describes the greenness or the density, and the health of the vegetation, based on the measurements of absorption and reflectance. The NDVI was calculated from MODIS MOD09Q1 V006 images on the basis of spectral reflectance from the soil-vegetation surface in the visible red (Band 1) and near-infrared (Band 2) spectra of electromagnetic waves according to:

$$NDVI = (R_{NIR} - R_{RED})/(R_{NIR} + R_{RED}), \quad (1)$$

where: R_{RED}—spectral reflectance in the red spectrum, R_{NIR}—spectral reflectance in the near-infrared spectrum. The values of spectral reflectance were the ratios of the reflected radiation over the incoming radiation in each spectral channel individually (albedo); hence, the NDVI takes on values between 0–1.

2.4.2. Statistical Analyses.

Statistical analyses were completed in STATISTICA software using the following quality measures: Pearson's correlation, Kendall's tau correlation, R (correlation coefficient), R^2 (coefficient of determination), MAPE (Mean Absolute Percentage Error), MPE (Mean Percentage Error), RMSE (Root Mean Square Error), and MBE (Mean Bias Error). The data were checked for the normal distribution and significance prior to all analyses. Validation of the retrieved SM values against the in situ measurements was preformed based on the RMSE error.

3. Results

3.1. Correlation between σ° Calculated from S-1 and Soil Moisture Measured at Different Depths

The in situ data and satellite data were used in statistical analyses to develop an inversion approach for the estimation of soil moisture from the Sentinel-1 data over the grassland and marshland sites.

Table 2 presents the results of Pearson's correlation (R values) for the marshland site between the backscattering coefficient (σ°) in the polarizations VH and VV, as calculated from Sentinel-1 (S-1), and the soil moisture (SM) when measured in situ at three depths: 5, 10, and 20 cm. The values came the dates of 26 April, 2015 to 30 June, 2017. Table 3 presents the same values for grassland site. The highest correlation was noted for the S-1 track 131 (ascending pass, low local incidence angles) and the soil moisture as measured at a 5 cm depth. The values of the correlation coefficient in any case were not higher than 0.59 for the marshland site and 0.72 for the grassland site.

For further analysis, the orbit pass ascending (A), and the depth of the soil moisture measurements at a 5 cm depth were taken into account (the highest correlation was found for these dataset).

Preprints (www.preprints.org) | NOT PEER-REVIEWED | Posted: 19 October 2018 doi:10.20944/preprints201810.0453.v1

Peer-reviewed version available at Remote Sens. 2018, 10, 1979; doi:10.3390/rs10121979

Table 2. Pearson's correlation (R values) for the marshland site between σ° VH and VV from S-1 and soil moisture (GS3), measured in situ at three depths: 5, 10, and 20 cm.

Marshland 2015-2017 Pearson correlation (R)						
Sentinel-1			Soil moisture GS3			Number of observations
Polarization	Track	Orbit pass	5 cm	10 cm	20 cm	N
VH	153	D[1]	0.49	0.34	0.40	57
	29	A[2]	0.51	0.39	0.49	70
	131	A[2]	0.56	0.46	0.59	66
VV	153	D[1]	0.47	0.27	0.36	57
	29	A[2]	0.40	0.22	0.28	70
	131	A[2]	0.55	0.39	0.52	66

[1] Descending, [2] Ascending.

Table 3. Pearson's correlation (R values) for the grassland site between σ° VH and VV from S-1, and soil moisture (GS3) measured in situ at three depths: 5, 10, and 20 cm.

Grassland 2015-2017 Pearson correlation (R)						
Sentinel-1			Soil moisture GS3			Number of observations
Polarization	Track	Orbit pass	5 cm	10 cm	20 cm	N
VH	153	D[1]	0.48	0.48	0.48	67
	29	A[2]	0.47	0.49	0.49	79
	80	D[1]	0.28	0.29	0.27	73
	131	A[2]	0.55	0.53	0.47	72
VV	153	D[1]	0.54	0.53	0.46	67
	29	A[2]	0.58	0.58	0.50	79
	80	D[1]	0.39	0.37	0.26	73
	131	A[2]	0.72	0.69	0.55	72

[1] Descending, [2] Ascending.

3.2. Impact of Vegetation on σ° Calculated from S-1 under Different Soil Moisture Conditions

It was noted that there was a different contribution from the vegetation, as represented by the NDVI, when there were dry conditions (SM<30%) or moist conditions (SM>60%). Figures 4–5 show the results of the statistical analyses that were performed between the backscattering coefficient (σ°) value as calculated from S-1 VH, and the NDVI as calculated from MODIS for the grassland site. Figure 4 presents the relationship between the σ° value and the NDVI for high, i.e. SM>60%, soil moisture when measured at a 5 cm depth. In this case, the vegetation played a role in the process of attenuation when the wave penetrated the vegetation to reach the soil. A different situation was observed when the soil was dry, i.e. SM<30%, at a 5 cm depth (Fig. 5). The impact of vegetation on the σ° S-1 VH was stronger than the impact of soil moisture. Higher biomass values were represented by the NDVI, and hence a higher amount of vegetation moisture content dominated the influence of vegetation on the σ° values. Under low SM conditions, an increase in the NDVI values caused an increase in the σ° S-1 VH values, while under high SM conditions, an increase of NDVI values caused a decrease in the σ° S-1 VH values.

Peer-reviewed version available at Remote Sens. 2018, 10, 1979; doi:10.3390/rs10121979

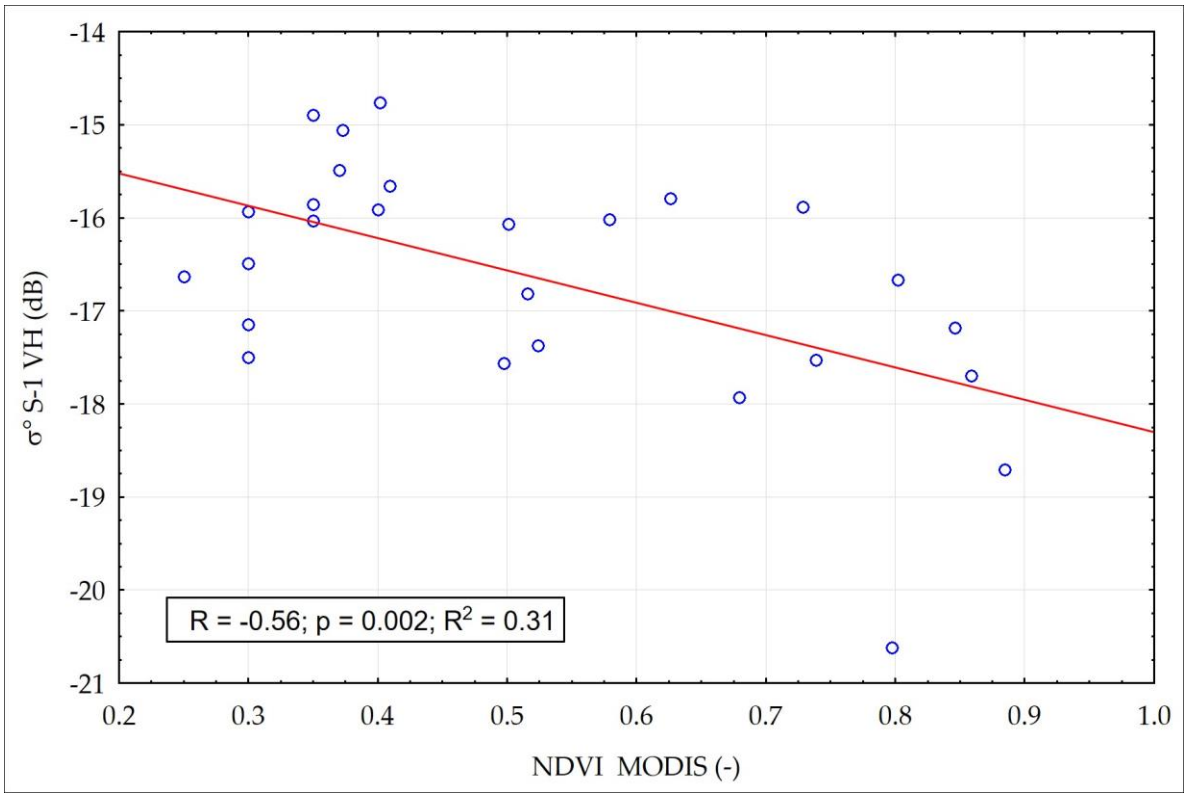

Figure 4. Relationship between the NDVI and σ° S-1 VH for the SM values measured at a 5 cm depth >60 vol. % at the grassland site.

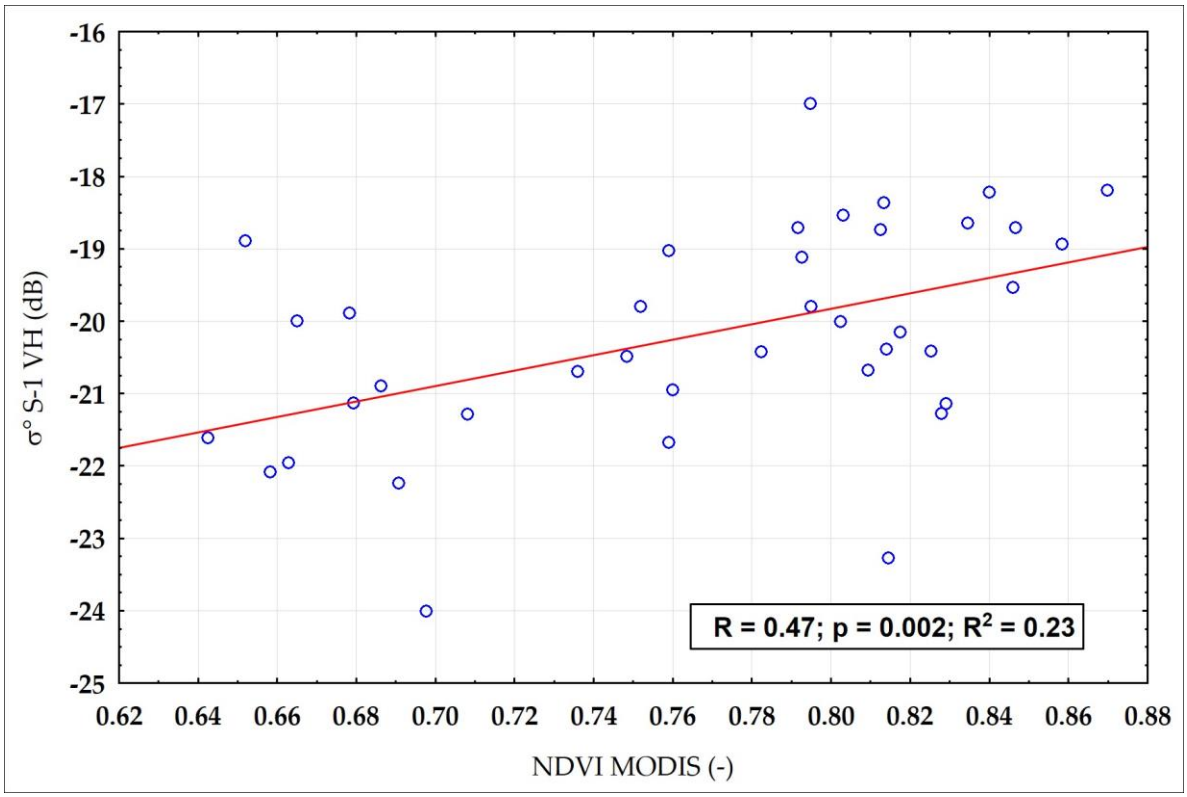

Figure 5. Relationship between the NDVI and σ° S-1 VH for the SM values measured at a 5 cm depth <30 vol. % at the grassland site.

3.3. Impact of Soil Moisture on σ° Calculated from S-1 under a Quasi-Constant NDVI

If the amount of marshland/grassland vegetation biomass represented by the NDVI is constant within a month, the variability of σ° S-1 is consistent with the variability of the soil moisture. Experimental data for the NDVI were gathered for each month separately, and the regression equation between the SM that was measured at a 5 cm depth, and σ° S-1 for each month of the growing season (March–November) was estimated. The obtained correlation coefficient between the soil moisture, and σ° S-1 VH and VV were high (Tab. 4). It was assumed that during the month, the vegetation biomass did not vary significantly, which was confirmed by the NDVI values that were observed during the months from March–November (Tab. 4). Also, the low standard deviations values (Tab. 4) for the NDVI for the particular months also indicated that the vegetation conditions did not vary during the month. Therefore, it can be assumed that the variability of the backscatter responds to the variability of the soil moisture in areas with homogeneous vegetation cover.

Table 4. Correlations between σ° S-1 VH and S-1 VV and SM at a 5 cm depth for the grassland and marchland sites during the seasons of 2015–2016.

Month	NDVI		SM at 5 cm and σ° S-1 VH			SM at 5 cm and σ° S-1 VV		
	Mean	St. dev.[1]	R^2	p-value	N[3]	R^2	p-value	N[3]
March	0.35	0.04	0.94	0.0001	10	0.93	0.0001	10
April	0.43	0.09	0.95	0.0000	10	0.95	0.0000	10
May	0.61	0.12	0.85	0.0002	13	0.93	0.0000	13
June	0.72	0.11	0.85	0.0038	9	0.88	0.0017	9
July	0.76	0.07	0.69	0.0060	14	0.40	0.1619	14
August	0.78	0.08	0.76	0.0045	12	0.75	0.0048	12
September	0.77	0.05	0.62	0.0230	13	0.44	0.1289	13
October	0.64	0.11	0.83	0.0000	21	0.73	0.0002	21
November	0.36	0.09	0.54	0.1086	10	0.25	0.4854	10

[1] Standard deviations, [2] Correlation coefficient, [3] Number of observations.

3.4. Compatibility of Seasonal Trends in the Course of the Vegetation Descriptor NDVI, and the σ° Difference VH–VV and Ratio VV/VH

The time series of σ° indices that were calculated as the difference of polarization VH–VV, or the ratio VV/VH, presented seasonality trends, i.e. variations that were specific to a particular timeframe. There was a systematic increase of NDVI values and σ° VH–VV during the vegetation season, and a decrease in autumn. Figure 6 presents the temporal evolution of the NDVI and σ° VH–VV values during the vegetation season in 2016 at the grassland test site as an example. Mann-Kendall tau statistics were performed for both sites for the seasons of 2016–2017 separately. It revealed that the compatibility of the seasonal trends of σ° VH–VV and VV/VH with the NDVI from MODIS MOD09Q1 V006 images were statistically sufficient (Tab. 5).

Preprints (www.preprints.org) | NOT PEER-REVIEWED | Posted: 19 October 2018 doi:10.20944/preprints201810.0453.v1

Peer-reviewed version available at Remote Sens. 2018, 10, 1979; doi:10.3390/rs10121979

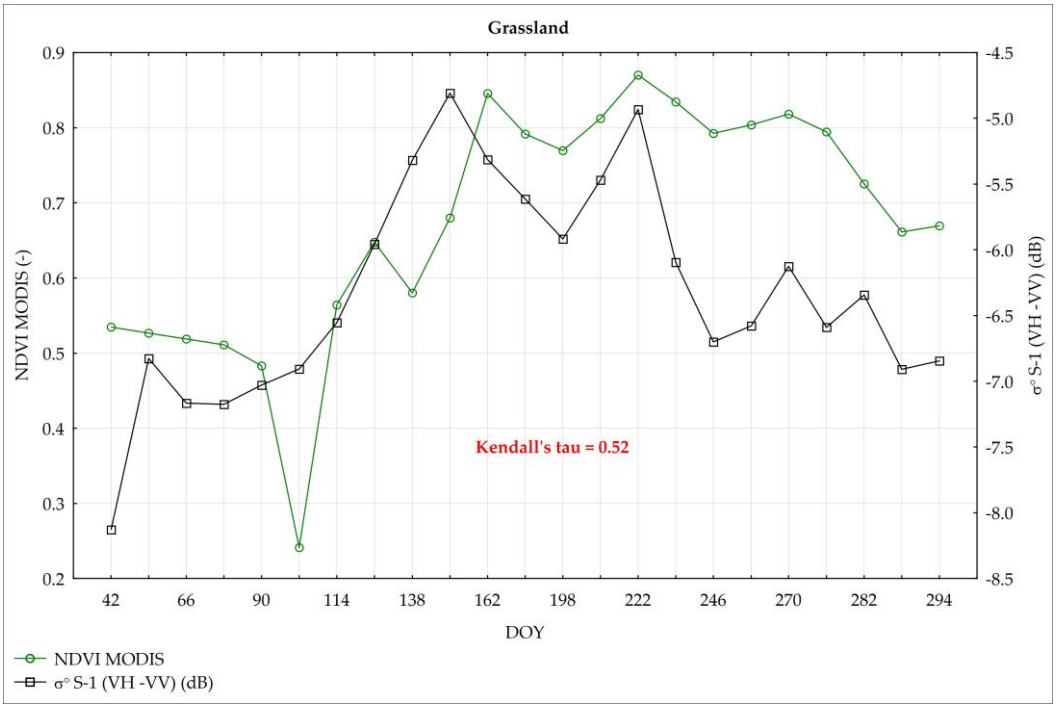

Figure 6. Temporal evolution of the NDVI and σ° S-1 VH−VV during the vegetation season of 2016 on the grassland site.

Table 5. Kendall's tau statistics between the NDVI and the σ° S-1 indices VH−VV and VV/VH for the grassland and marshland sites.

Site	Year	S-1 track	Kendall's tau for VH-VV	N[1]	Kendall's tau for VV/VH
grassland	2016	29	0.52	37	0.42
		131	0.39	36	0.46
	2017	29	0.51	27	0.28
		131	0.50	26	0.28
marshland	2016	29	0.35	37	0.37
		131	0.54	36	0.56
	2017	29	0.68	27	0.39
		131	0.74	25	0.32

[1] Number of observations.

It has been assumed that the influence of vegetation on σ° S-1 values could be expressed by indices of the difference between σ° VH and VV (VH−VV) and the ratio of σ° VV/VH. Analyzing Kendall's tau coefficients for all test sites, tracks, and seasons, it was found that both σ° S-1 VH−VV and σ° S-1 VV/VH indexes were in monotonic correlation with the NDVI, and that they could replace the NDVI values in soil moisture modeling. In the experiment, the values of σ° S-1 VV/VH was always positive and less than 1.

By applying the indices calculated using the S-1 data in modeling SM, the independance from the optical data (often overcast conditions) was ensured. Also, it allowed for quick calculations of soil moisture, which often changes rapidly and has to be observed regularly.

The two following approaches are presented in building the model for soil moisture retreivement:

1. Using the NDVI as a vegetation descriptor
2. Substituting the NDVI by the index σ° S-1 VH−VV and the index σ° S-1 VV/VH

3.5. Soil Moisture Retrieval using σ° from Sentinel-1 and NDVI from MODIS.

Water Cloud Model with the Least Square Regression Method

The water cloud model represents the total backscatter from the canopy σ^o as the sum of the contribution of the vegetation σ^o_{veg} and of the underlying soil σ^o_{soil} [32]:

$$\sigma^o = \sigma^o_{veg} + \tau^2 \sigma^o_{soil} \quad (2)$$

where:

$$\sigma^o_{veg} = A \cdot V_1^E \cos(\theta) (1-\tau^2) \quad (3)$$

$$\tau^2 = \exp(-2B \cdot V_2/\cos(\theta)) \quad (4)$$

where: θ—incidence angle, τ^2—two way attenuation through the canopy: V_1 and V_2 are descriptors of the canopy, A and B are fitted parameters of the model that depend on the vegetation descriptor and the radar configuration. The $\sigma°_{soil}$ is a linear function of soil moisture.

As the vegetation descriptors (V_1 and V_2), the NDVI values were taken from the MODIS data.

The signal from soil moisture is attenuated by the vegetation:

$$\tau^2 = \exp(-NDVI/\cos(\theta)) \quad (5)$$

The following two components were designed to describe the effect of the vegetation and the underlying soil on *σ°* S-1 *VH* value—$\sigma°_{soil}$: τ^2*SM and $\sigma°_{veg}$: $(1-\tau^2)$*cos(θ)*NDVI. The first component, $\sigma°_{soil}$, represents the interaction of the incident radiation between the vegetation and the underlying soil. τ^2 reduces the impact of the soil on backscatter when the covered vegetation is dense and increases. τ^2 takes the value from 0–1 and is inversely proportional to the vegetation index and to the incidence angle. The second component, $\sigma°_{veg}$, describes the part of the backscatter that depends on the vegetation canopy covering the soil.

The parameters of the model with σ° Sentinel-1 VH as a dependent variable, and $\sigma°_{soil}$ and $\sigma°_{veg}$ as independent variables, were estimated by applying the least squares regression method. Data were limited to the vegetation season, i.e. from 60–300 days of each year.

Model 1a:

$$\sigma° \text{ S1VH} = -28.3 + 0.2*\tau^2*SM + 14.7*(1-\tau^2)*\cos(\theta)*NDVI \quad (6)$$

where: R = 0.92; R^2 = 0.85; p<0.0000; N = 147; Std. Err. = 0.79 dB.

The partial correlation for the soil and vegetation components were 0.89 and 0.54 respectively, which means that soil moisture influenced σ° S-1 VH more strongly than did the vegetation cover. Figure 7 presents a comparison between the observed values of σ° S-1 VH (derived from S-1 images) and those that were predicted using Model 1a (Eq. 6).

Preprints (www.preprints.org) | NOT PEER-REVIEWED | Posted: 19 October 2018 doi:10.20944/preprints201810.0453.v1

Peer-reviewed version available at Remote Sens. 2018, 10, 1979; doi:10.3390/rs10121979

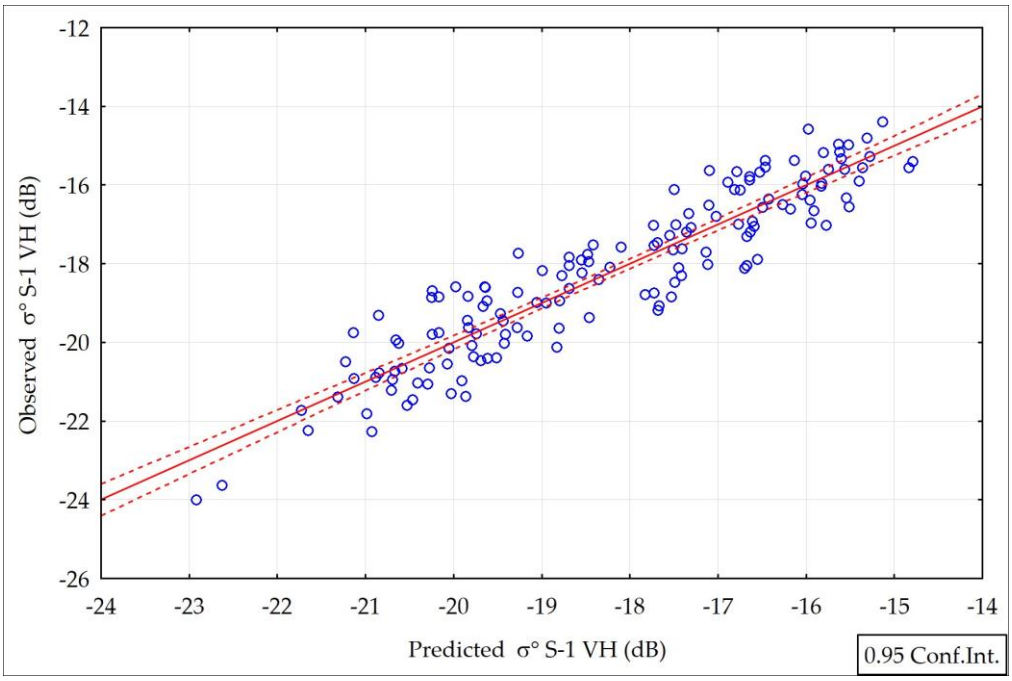

Figure 7. The σ° S-1 VH values observed and predicted by Model 1a (Eq. 6).

Model 1b:

$$\sigma^\circ \text{ S-1 VV} = -21.5 + 0.19^* \tau^2 * SM + 12.3^*(1-\tau^2)^*\cos(\theta)^*NDVI \quad (7)$$

where: R = 0.91; R^2 = 0.82; p<0.0000; N = 170; Std. Err. = 0.84 dB.

The partial correlation for the soil and vegetation components were 0.87 and 0.50 respectively, which means that soil moisture influenced σ° S-1 VV more strongly than did the vegetation cover. Figure 8 presents a comparison between the σ° S-1 VV values observed (derived from satellite images) and predicted by Model 1b according to Equation 7.

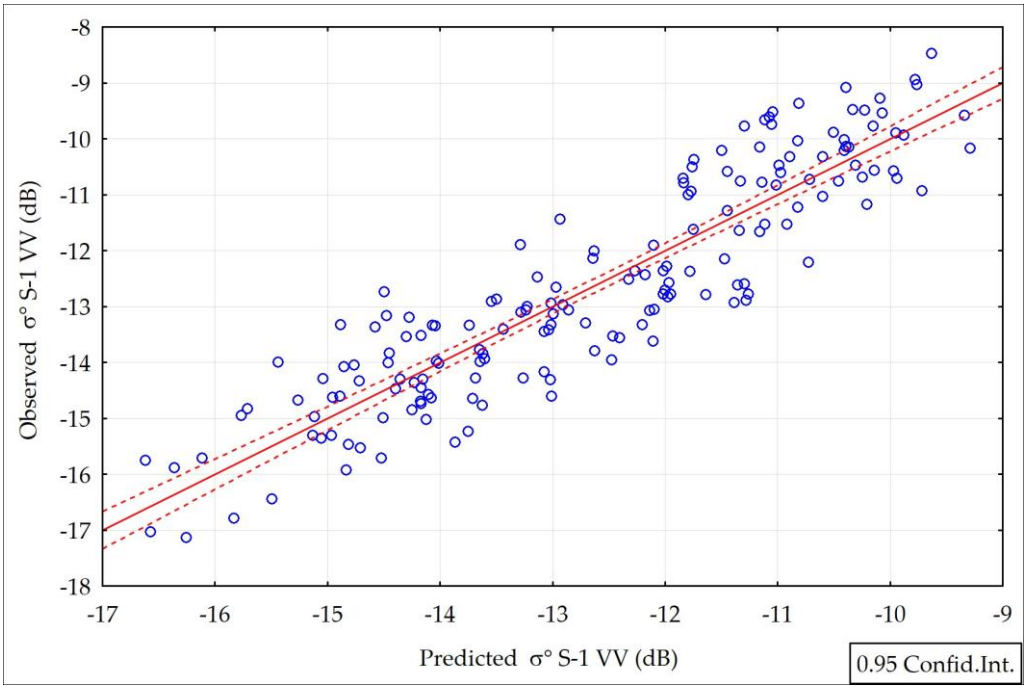

Figure 8. The σ° S-1 VV values observed and predicted by Model 1b (Eq. 7).

Preprints (www.preprints.org) | NOT PEER-REVIEWED | Posted: 19 October 2018 doi:10.20944/preprints201810.0453.v1

Peer-reviewed version available at Remote Sens. 2018, 10, 1979; doi:10.3390/rs10121979

The models 1a–1b present the influence of soil moisture and vegetation cover (expressed by NDVI from MODIS) on the S-1 backscatter. The standard errors of estimation for σ° S1VH and σ° S1 VV were 0.79 dB and 0.84 dB, respectively.

Table 6 presents the mean absolute percentage errors (MAPE) of the σ° S-1 ascending pass, assessed by Model 1a and Model 1b for the years 2015–2017 for the two sites and the two tracks separately. MAPE1 applies to Model 1a, and MAPE2 applies to Model 1b. The mean percentage error for σ° S-1 VH estimation was 6.6%, and for σ° S-1 VV estimation, it was 8.8% for all observations. The distribution of the error was well balanced on the sites and the tracks.

Table 6. Mean absolute percentage error (MAPE) errors of σ° S-1 VH and VV derived from Model 1a and Model 1b for the years 2015–2017.

Site	Track	MAPE1[1] (%)	MAPE2[2] (%)	Number of observations
Grassland	131	5.7	8.7	62
	29	5.9	8.8	56
Marshland	131	7.6	8.8	45
	29	7.2	8.8	47
All		6.6	8.8	200

[1] Errors applies to Model 1a, [2] Errors applies to Model 1b.

Figures 9–10 present the simulation of σ° S1 VH and σ° S1 VV with the increase of the NDVI for various values of soil moisture from the range of 10–90 vol. %. The increase of σ° with the increase of the NDVI was significant with low soil moisture. When the soil moisture was high, the increase of the NDVI did not influence the increase of σ°.

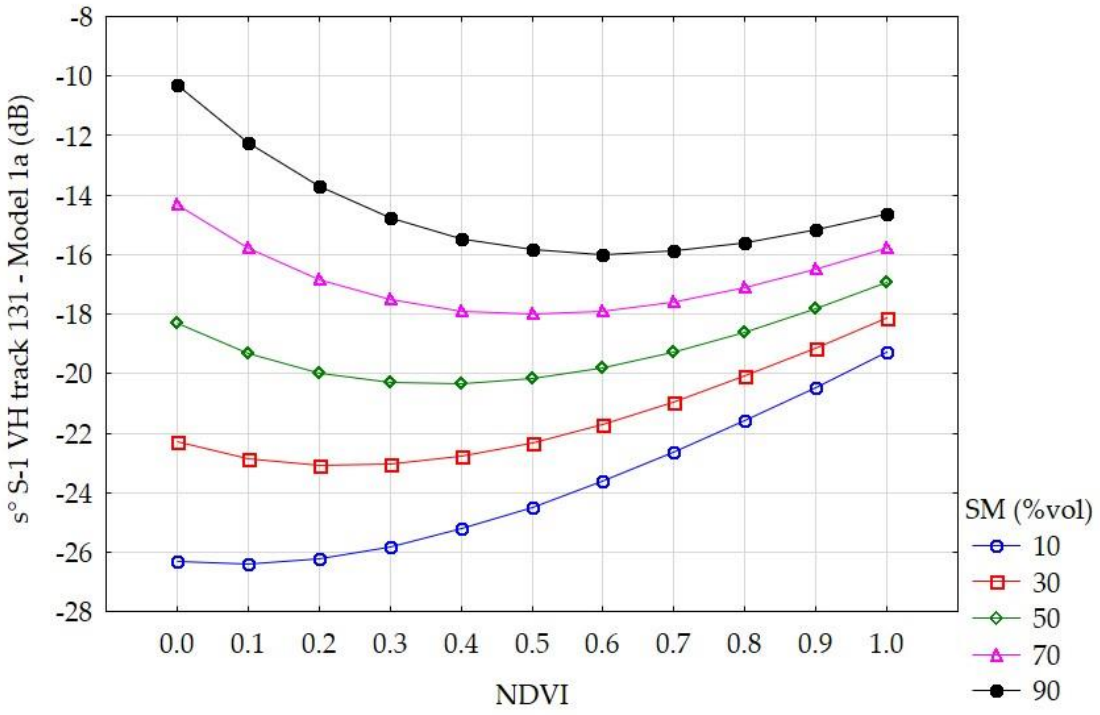

Figure 9. Impact of NDVI on σ° S-1 VH under various levels of soil moisture (SM) according to Model 1a.

Preprints (www.preprints.org) | NOT PEER-REVIEWED | Posted: 19 October 2018 doi:10.20944/preprints201810.0453.v1

Peer-reviewed version available at Remote Sens. 2018, 10, 1979; doi:10.3390/rs10121979

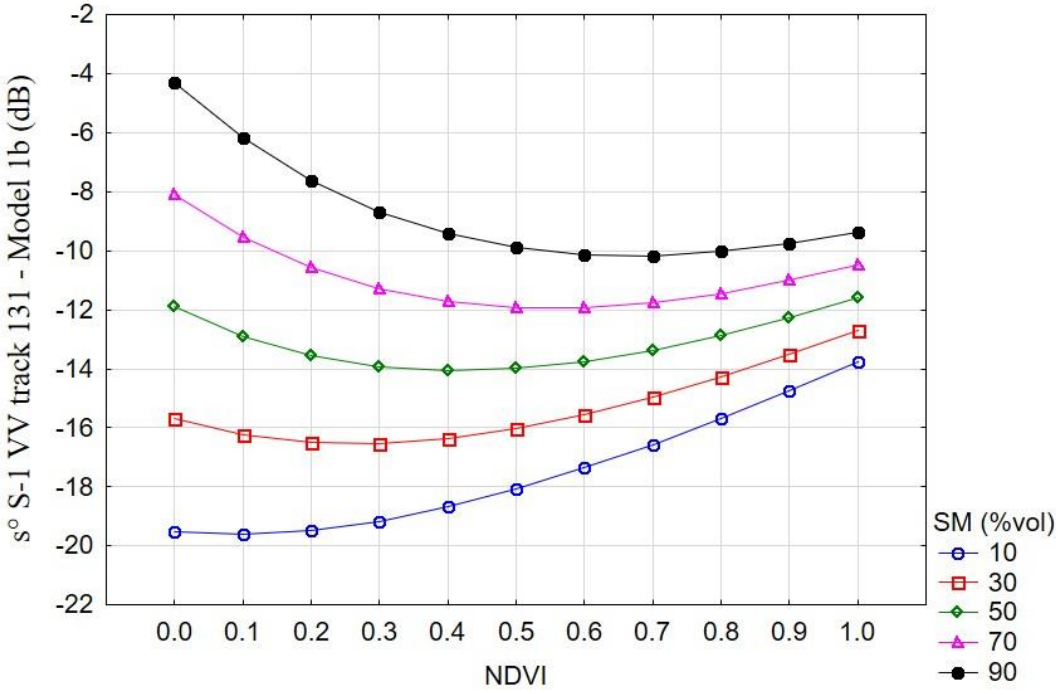

Figure 10. Impact of NDVI on σ° S-1 VV under various levels of soil moisture according to Model 1b.

The soil moisture can be retrieved through the inversion of Model 1a (Eq. 6) with an accuracy of 9.8 vol. % (Eq. 8). The errors were similar for two sites.

$$SM = (S\text{-}1\ \sigma^\circ\ VH + 28.3 - 14.7 * (1-\tau^2) * \cos(\theta) * NDVI) / (0.2 * \tau^2) \quad (8)$$

Table 7 presents the RMSE errors (vol. %) for selected ranges of soil moisture values (5 cm depth) based on Model 1a. It was noted that for the high SM values (in the range of 80–100 vol %) errors were lower than those of the remaining SM ranges.

Table 7. Errors of soil moisture retrieval by Model 1a (ascending pass) 2015–2017.

SM range	N[1]	RMSE (vol %)
20 - 40	39	11.8
40 - 60	39	9.5
60 - 80	35	9.9
80 - 100	34	8.4
All	147	9.8

[1] Number of observations.

Table 8 presents the RMSE errors (vol %) for selected ranges of the NDVI values based on Model 1a. The RMSE errors were between 7.4–11.5 vol. %. It was clearly visible that the error was higher with denser vegetation cover (higher NDVI values).

Table 8. Errors of soil moisture retrieval by Model 1a for different densities of vegetation.

NDVI range	N[1]	RMSE (vol %)
0.2 – 0.4	24	7.4
0.4 – 0.6	40	8.5
0.6 – 0.8	47	10.4
0.8 – 0.9	36	11.5
All	147	9.8

[1] Number of observations.

Preprints (www.preprints.org) | NOT PEER-REVIEWED | Posted: 19 October 2018 doi:10.20944/preprints201810.0453.v1

Peer-reviewed version available at Remote Sens. 2018, 10, 1979; doi:10.3390/rs10121979

3.6. Soil Moisture Retrieval using the σ° Index from Sentinel-1.

Water Cloud Model with the Least Squares Regression Method.

Let us assume that:

$$\tau^2 = \exp(-2(\sigma^\circ \text{ S-1 VV/VH})/\cos(\theta)) \quad (9)$$

where: σ° S-1 VV and VH had the only negative values in our study, and σ° S-1 VV/VH <1. Two components were designed to describe the effect of the underlying soil and vegetation on the Sentinel-1 value—σ°_{soil}: τ^2*SM and σ°_{veg}: $(1 - \tau^2)$*cos(θ)*σ° S-1 $(VH-VV)^2$. Then, σ° S-1 VH was modeled according to Model 2.

Model 2

$$\sigma^\circ \text{ S-1 VH} = -18.9 + 0.33*\sigma^\circ_{soil} - 0.14*\sigma^\circ_{veg} \quad (10)$$

This gives the equation:

$$\sigma^\circ \text{ S-1 VH} = -18.9 + 0.33\ \tau^2*SM - 0.14*(1- \tau^2)*\cos(\theta)*\sigma^\circ \text{ S-1 } (VH-VV)^2 \quad (11)$$

where: R = 0.91; R^2 = 0.82; p<0.000; N = 252; Std. Err. = 0.70 dB, (Fig. 11).

There is no redundancy of independent variables in the multiple regression model. The correlation between them is R^2=0.002.

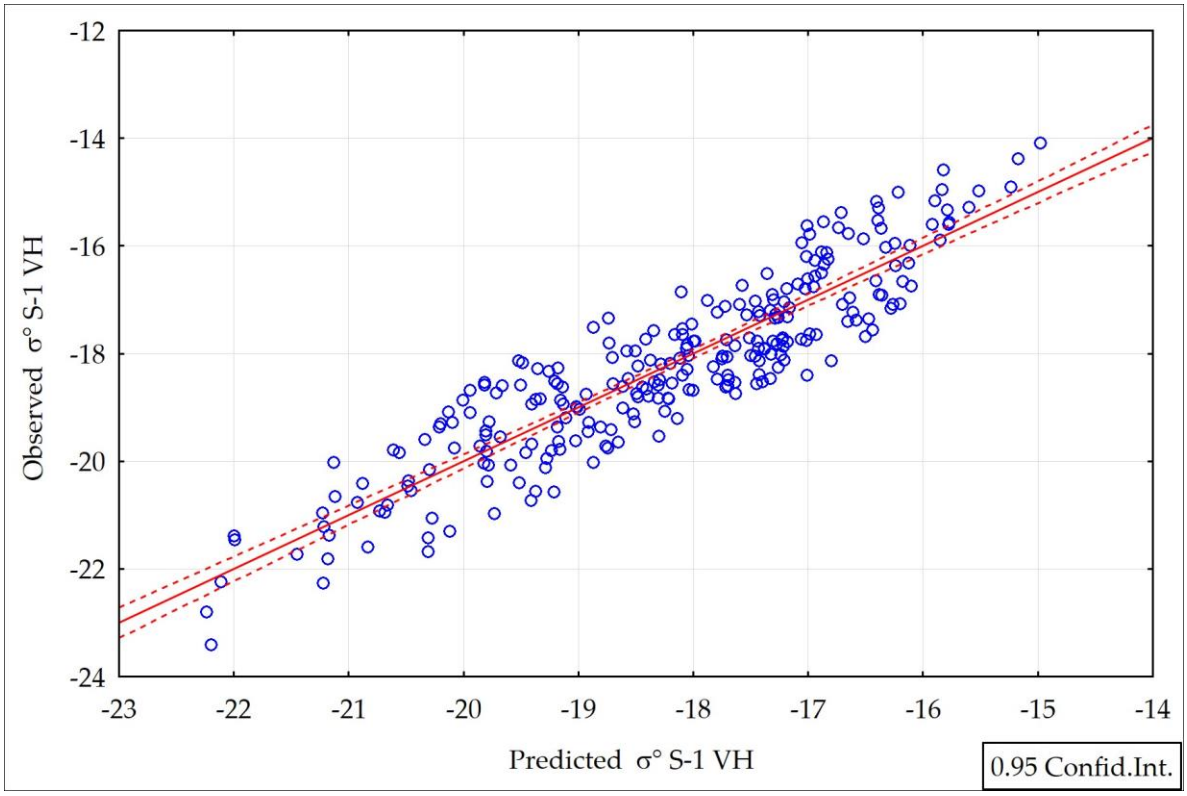

Figure 11. The σ° S-1 VH values observed and predicted by Model 2 (Eq. 11).

From the Model 2 inversion, the soil moisture was calculated as follows:

$$SM = (\sigma^\circ \text{ S-1 VH} + 18.9 - 0.14*(1- \tau^2)*\cos(\theta)*\sigma^\circ \text{ S-1 } (VH-VV)^2 / (0.33* \tau^2) \quad (12)$$

The mean RMSE error of the soil moisture retrieved from Model 2 (Eq. 12) was 13 vol. % (Tab. 9–10). Table 9 presents the RMSE errors from data for the whole year when the soil temperature is >278 °K.

Peer-reviewed version available at Remote Sens. 2018, 10, 1979; doi:10.3390/rs10121979

Table 10 presents the RMSE errors for the data from the vegetation season, i.e. from the DOY (Day Of the Year) 60–300.

Table 9. Errors analysis for different ranges of SM (5 cm depth) as retrieved by Model 2 (whole year).

SM range (vol. %)	N[1]	RMSE (vol. %)
20 - 40	51	14.8
40 - 60	53	11.8
60 - 80	64	13.8
80 - 100	40	13.6
All	252	13.0

[1] Number of observations.

Table 10. Errors analysis for different ranges of SM (5 cm depth) as retrieved by Model 2 (vegetation season).

SM range (vol. %)	N[1]	RMSE (vol. %)
20 - 40	60	12.1
40 - 60	70	12.3
60 - 80	60	14.7
80 - 100	62	11.8
All	208	13.5

[1] Number of observations.

The validation of Model 2 was performed for the S-1 data between September 2017–May 2018. The data from December–March were excluded, as the soil temperatures were lower than 278 °K. Table 11 presents the RMSE errors for the data used in the validation procedure.

Table 11. Errors analysis for different ranges of SM (5 cm depth) retrieved by Model 2 for validation data.

SM range (vol. %)	N[1]	RMSE (vol. %)
40 - 60	14	11.0
60 - 80	29	8.5
80 - 100	35	15.2
All	76	12.6

[1] Number of observations.

For S-1 satellite track 29, where the incident angle was higher than for track 131, all of the models gave higher errors of soil moisture estimation. Table 12 presents the mean RMSE errors for both of these tracks separately.

Table 12. Errors of soil moisture estimation from developed models for two satellite tracks.

Orbit/Track	Model 1a	Model 1b	Model 2
		RMSE (vol %)	
A/29	10.0	10.8	15.2
A/131	9.5 l	9.9	10.7

Figures 12–13 present a comparison between the soil moisture retrieved by the Model 2 inversion according to Equation 12, and the soil moisture measured at a 5 cm depth by the Decagons GS3 sensors at the grassland and marshland sites. As can be seen in the figures, high compatibility occurred between the SM values that were modeled and measured; however, this was higher for the marshland site. The lack of response of the Decagon probes to precipitation during the extreme drought in June to Sep of 2015 can be explained by the hydrophobic effect of the dry peat [33]. The

time of reaction of the soil moisture and the retention of water in the soil on precipitation in peat soils is much slower than in other soils. After the precipitation that occurred in July and at the beginning of August 2017, the soil moisture has raised in the middle of August at the grassland site and at the end of August at the marshland site.

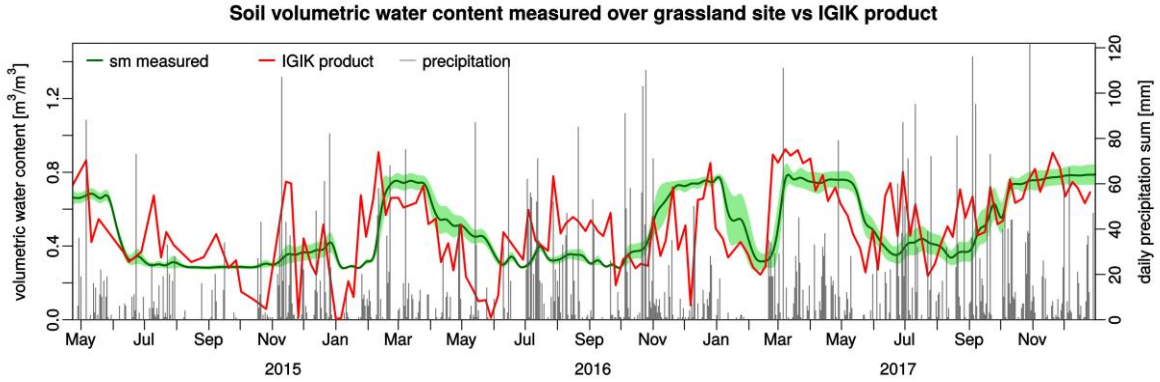

Figure 12. Comparison between the soil moisture retrieved by the inversion of Model 2 according to Equation 12 (IGiK (Institute of Geodesy and Cartography) product) and soil moisture measured at a 5 cm depth (sm) by the Decagons GS3 sensors at the grassland site.

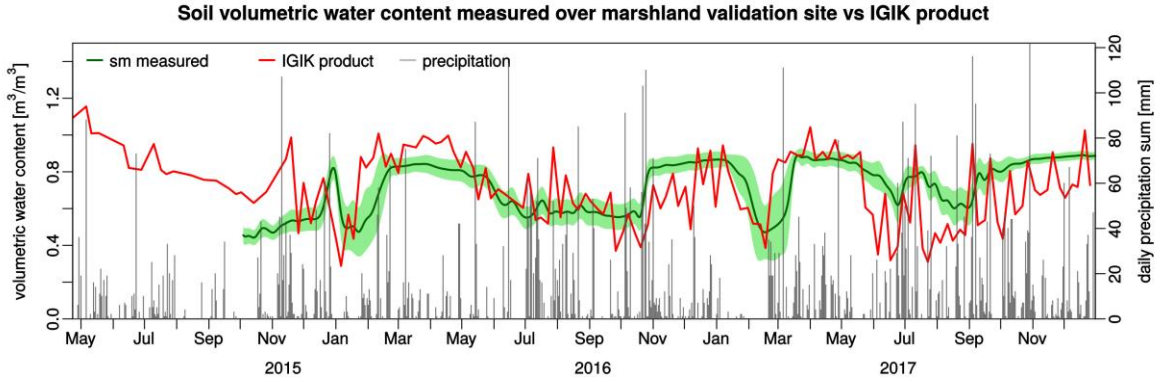

Figure 13. Comparison between the soil moisture retrieved by the inversion of Model 2 according to Equation 12 (IGiK (Institute of Geodesy and Cartography) product), and soil moisture measured at a 5 cm depth (sm) by the Decagons GS3 sensors at the marshland site.

4. Discussion

Although previous studies have identified relationships between S-1 σ° and the surface soil moisture [16, 17, 18, 19, 23], this study, for the first time, to our knowledge, in the Biebrza Wetlands, demonstrates the relationships under an extreme range of SM conditions (from dry to wet) i.e. 27–90 vol. %, and different wetland vegetation biomasses (NDVI). The moisture ranges presented, and the diversity of the vegetation biomass, depicts the wetland ecosystems well. The developed models for soil moisture retrieval could be implemented into the system for monitoring areas of wetlands, and in developing decision support and early warning systems.

Two models have been developed based on σ° S-1 VH and VV, and the NDVI from MODIS. It is evident in Table 6 that for both sites (grassland and marshland) when considered together, the MAPE errors of σ° as modeled by Model 1a (Eq. 6) and Model 1b (Eq. 7) are comparable; however, for Model 1b, they are slightly higher. Generally, the inversion of the developed σ° models can retrieve the SM with a mean accuracy that is close to 10 vol. %, which is acceptable for the wetland ecosystem authorities and the decision makers. This is especially important for the wetlands areas that are not easily accessible.

The σ° S-1 indices as VH−VV and VV/VH, which could replace the vegetation cover as expressed by the NDVI values in soil moisture modeling, have been used to develop Model 2 (Eq. 11). Inversion

of Model 2 (Eq. 12) allows the soil moisture to be retrieved by solely using Sentinel-1 data with a mean accuracy of 13 vol. % (Tab. 9). Although the accuracy of the soil moisture retrieval using Model 2 was slightly lower than applying Models 1a and 1b, it was still acceptable. Moreover, Model 2 required only microwave data, which is advantageous, especially in areas that are often cloudy.

5. Conclusions

The study has shown that the retrieval of soil moisture based on Sentinel-1 data, which considers wetland ecosystems, can be used effectively and with reasonable accuracy (below 10 vol. %). These developments are valuable for areas where in situ data are not available due to the inaccessibility of the area, and when only satellite data can provide suitable tools for decision makers.

The setup of two dense soil moisture measuring networks located over the wetlands offered unprecedented capabilities for modeling the soil moisture from the Sentinel-1 data. The data collected within the study corresponded to from extremely dry (2015) to extremely wet (2017) conditions, which is favorable for the development and validation of soil moisture retrieval models over the wetlands. Also, the selected grassland and marshland sites feature different soil moisture regimes.

Vegetation has to be considered in the relationship between the backscatter and the soil moisture. The vegetation contribution could be expressed by NDVI, or by VV/VH and VH−VV indices that are calculated from the S-1 data.

It has been noted that there is a different contribution of vegetation that is represented by the NDVI when there are dry conditions (SM<30 vol. %) and moist conditions (SM>60 vol. %). It was noticed that the values from 50–60 vol. % of soil moisture are within the threshold for the SM influence on σ° S-1 VH and VV.

There are discrepancies between Sentinel-1A and Sentinel-1B data. Ascending orbits are better for soil moisture retrieval because the descending overpasses occur during the night when there is dew. The most significant correlation coefficients between the S-1 backscatter and the soil moisture were found for the ascending tracks and for 5 cm depths. A validation was performed for the period of September 2017 until May 2018. The average error was close to 12.6%. It has to be emphasized that the extent of the soil moisture in the wetlands was high, at 27–90%. Such a moisture extent does not occur in agriculture sites. This could also affect the range of the error.

Developed models could be applied for sites other than the European Wetlands.

Further work is needed, especially when HH polarization of S-1 is available, to predict the moisture status in wetland ecosystems. The time of reaction of soil moisture and retention of water on precipitation in peat soil was much slower than the reaction on precipitation of other soils. That is why it will be good to examine the time of reaction of SM on precipitation in peat soil.

Acknowledgments: The study was funded by ESA EXPRO, contract no. 4000112578/14/NL/MP "Biebrza Sentinel-1 Supersite", and the National project Narodowe Centrum Nauki 2016/23/B/ST10/03155.

Author Contributions: Katarzyna Dabrowska–Zielinska conceived and designed the experiments and wrote the paper; Jan Musial performed the experiments established the soil moisture network over the Biebrza Wetlands and processed microwave satellite data; Alicja Malinska performed statistical analyses; Maria Budzynska analyzed the data and contributed in writing the paper; Radoslaw Gurdak performed the in situ experiments; Wojciech Kiryla processed and analyzed the optical satellite data; Maciej Bartold established the in situ measurements; Patryk Grzybowski performed the database analysis.

Conflicts of Interest: The authors declare no conflict of interest.

References

1. https://www.biebrza.org.pl/lang,2
2. Turbiak, J., Miatkowski, Z. Assessment of organic mass mineralization rate in deeply drained peat-muck soil based on losses of soil mass and CO2 emission. ITP Water Environ. Rural Areas, 2016 (VII–IX), 16, (3) (55), 73-85, www.itp.edu.pl/wydawnictwo/woda.
3. Huang, W., Hall, S. J. Elevated moisture stimulates carbon loss from mineral soils by releasing protected organic matter. Nature Communications, 2017, 8, Article number: 1774, DOI: 10.1038/s41467-017-01998.

4. Dembek, W.; Oswit, J.; Rycharski, M. Torfowiska i torfy w Pradolinie Biebrzy. In *Przyroda Biebrzanskiego Parku Narodowego,* A. Dyrcz, A., C. Werpachowski, C., Eds; Publisher: Biebrzanski Park Narodowy, Osowiec-Twierdza, Poland, **2005**; 33-58.
5. Kornelsen K. C.; Coulibaly, P. Advances in soil moisture retrieval from synthetic aperture radar and hydrological applications. *J. Hydrol.*, **2013,** *476*, 460–489, https://doi.org/10.1016/j.jhydrol.2012.10.044.
6. Allen, C.T.; Ulaby, F.T. Modelling the Polarization Dependence of the Attenuation in Vegetation Canopies. Proceedings of the Geoscience and Remote Sensing Symposium (IGARSS'84), Strasbourg, 27-30 August 1984, 119-124.
7. Le Toan, T.; Lopes, A.; Huet, M. On the relationships between radar backscattering Coefficient and Vegetation Canopy Characteristics. Proceedings of the Geoscience and Remote Sensing Symposium (IGARSS'84), Strasbourg, 27-30 August 1984, 155-160.
8. Attema, E.P.; Ulaby, F.T. Vegetation modeled as a water cloud. *Radio Science*, **1978**, 13, (2), 357-364.
9. Dabrowska–Zielinska, K.; Inoue, Y.; Kowalik, W.; Gruszczynska, M. Inferring the effect of plant and soil variables on C- and L-band SAR backscatter over agricultural fields, based on model analysis. *Adv. Space Res.*, **2007**, *39, (1)*, 139–148, DOI: 10.1016/j.asr.2006.02.032.
10. Mattia, F., Satalino, G., Dente, L., Pasquariello, G., 2006. Using a priori information to improve soil moisture retrieval from ENVISAT ASAR AP data in semiarid regions. IEEE Trans. Geosci. Remote Sens. 44 (4), 900–912.
11. Balenzano, A.; Satalino, G.; Pauvels, V.; Mattia, F. Soil moisture retrieval from dense temporal series of C-band SAR data over agricultural sites. Proceedings of the Geoscience and Remote Sensing Symposium (IGARSS), 2011 IEEE International, 24-29 July 2011, Vancouver, BC, Canada, DOI: 10.1109/IGARSS.2011.6049883.
12. Baghdadi, N.; El Hajj, M.; Zribi, M.; Fayad, I. Coupling SAR C-band and optical data for soil moisture and leaf area index retrieval over irrigated grasslands. *IEEE J. Sel. Top. Appl. Earth Obs. Remote. Sens.*, **2015**, *9 (3)*, 1-15, DOI: 10.1109/JSTARS.2015.2464698.
13. Baghdadi, N.; Choker, M.; Zribi, M.; El Hajj, M.; Paloscia, S.; Verhoest, N.; Lievens, H.; Baup, F.; Mattia, F. A new empirical model for Radar scattering from bare surfaces. *Remote Sens.*, **2016**, *8*, 920–934, DOI:10.3390/rs8110920.
14. Choker, M.; Baghdadi, N.; Zribi, M.; El Hajj, M.; Paloscia, S.; Verhoest, N.; Lievens, H.; Mattia, F. Evaluation of the Oh, Dubois and IEM models using large dataset of SAR signal and experimental soil measurements. *Water*, **2017**, *9 (38)*, 1–27, DOI:10.3390/w9010038.
15. Pasolli, L.; Notarnicola, C.; Bertoldi, G.; Bruzzone, L.; Remelgado, R.; Greifeneder, F.; Niedrist, G.; Della Chiesa, S.; Tappeiner, U.; Zebisch, M. Estimation of soil moisture in mountain areas using SVR technique applied to multiscale active radar images at c-band. IEEE J. Sel. Topics Appl. Earth Observ. Remote Sens. **2015**, 8, (1), 262–283, DOI: 10.1109/JSTARS.2014.2378795.
16. Mattia F.; Satalino G.; Balenzano A.; Pauwels V.; DeLathauwer E. GMES Sentinel-1 soil moisture retrieval algorithm development. European Space Agency contract n. 4000101352/10/NL/MP/ef, Final Report, 2011, November.
17. Balenzano, A.; Mattia, F.; Satalino, G.; Pauvels, V.; Snoeij, P. SMOSAR algorithm for soil moisture retrieval using Sentinel-1 data. Proceedings of the Geoscience and Remote Sensing Symposium (IGARSS), 2012 IEEE International, 22-27 July 2012, Munich, Germany, DOI: 10.1109/IGARSS.2012.6351332.
18. Paloscia, S.; Pettinanto, S.; Santi, E.; Notarnicola, C.; Pasolli, L.; Reppucci, A. Soil moisture mapping using Sentinel-1 images: algorithm and preliminary validation. *Remote Sens. Environ.*, **2013**, *134*, 234–248, http://dx.doi.org/10.1016/j.rse.2013.02.027.
19. Santi, E.; Paloscia, S.; Pettinato, S.; Fontanelli, G. Application of artificial neural networks for the soil moisture retrieval from active and passive microwave spaceborne sensors. *Int. J. Appl. Earth Obs. Geoinf.*, **2016**, 48, 61–73, http://dx.doi.org/10.1016/j.jag.2015.08.002.
20. Kasischke, E.; Bourgeau-Chavez, L.; Rober, A.; Wyatt, K.; Waddington, J.; Turetsky, M. 2009. Effects of soil moisture and water depth on ERS SAR backscatter measurements from an Alaskan wetland complex. *Remote Sens. Environ.*, **2009**, *113*, 1869–1873, DOI:10.1016/j.rse.2009.04.006.
21. Lang, M. W.; Kasischke, E. S.; Prince, S. D.; Pittman, K. W. Assessment of C-band synthetic aperture radar data for mapping and monitoring Coastal Plain forested wetlands in the Mid-Atlantic Region, U.S.A. *Remote Sens. Environ.*, **2008,** *112*, 4120–4130, DOI: 10.1016/j.rse.2007.08.026.

22. Santi, E.; Paloscia, S.; Pettinato, S.; Notarnicola, C.; Pasolli, L.; Pistocchi, A. Comparison between SAR Soil Moisture Estimates and Hydrological Model Simulations over the Scrivia Test Site. *Remote Sens.*, **2013**, *5*, 4961-4976, DOI:10.3390/rs5104961.
23. Dabrowska–Zielinska, K.; Budzynska, M.; Tomaszewska, M.; Malinska, A.; Gatkowska, M.; Bartold, M.; Malek, I. Assessment of Carbon Flux and Soil Moisture in Wetlands Applying Sentinel-1 Data. *Remote Sens.*, **2016**, *8*, 756, 1-22, DOI:10.3390/rs8090756.
24. Vreugdenhil, M.; Wagner, W.; Bauer-Marschallinger, B.; Pfeil, I.; Teubner, I.; Rüdiger, C.; Strauss, P. Sensitivity of Sentinel-1 Backscatter to Vegetation Dynamics: An Austrian Case Study. *Remote Sens.* **2018**, *10*, 1396, DOI:10.3390/rs10091396.
25. Greifeneder, F.; Notarnicola, C.; Hahn, S.; Vreugdenhil, M.; Reimer, C.; Santi, E.; Paloscia, S.; Wagner, W. The Added Value of the VH/VV Polarization-Ratio for Global Soil Moisture Estimations From Scatterometer Data. IEEE J. Sel. Topics Appl. Earth Observ. Remote Sens. 2018, 11, (10), 3668 - 3679, DOI: 10.1109/JSTARS.2018.2865185.
26. http://www.biebrza.org.pl/index.php
27. Silakowski, M. Charakterystyka fizyczno-geograficzna-Klimat. In *Biebrzanski Park Narodowy*, Sienko, A., Grygoruk, A., Eds.; Publisher: Biebrzanski Park Narodowy, Osowiec-Twierdza, Poland, **2003**; 17-22.
28. Musial, J.P.; Dabrowska-Zielinska, K.; Kiryla, W.; Oleszczuk, R;, Gnatowski, T.; Jaszczynski, J. Derivation and validation of the high resolution satellite soil moisture products: a case study of the Biebrza Sentinel-1 validation sites. *Geoinformation Issues*, **2016**, vol. 8, pp. 37-53.
29. Dorigo, W.; Wagner, W.; Hohensinn, R.; Hahn, S.; Paulik, C.; Xaver, A.; Gruber, A.; Drusch, M.; Mecklenburg, S.; Oevelen, P.V., et al. The International Soil Moisture Network: a data hosting facility for global in situ soil moisture measurements. *Hydrology and Earth System Sciences*, **2011**, 15, 1675-1698.
30. Vermote, E. MOD09Q1 MODIS/Terra Surface Reflectance 8-Day L3 Global 250m SIN Grid V006 [Data set]. NASA EOSDIS LP DAAC. 2015, DOI:10.5067/MODIS/MOD09Q1.006.
31. Rao, S.; Sahadevan, D.; Wadodkar, M.; Nagaraju, M.; Chattaraj, S.; Joseph, W.; Rajankar, P.; Sengupta, T.; Venugopalan, M.; Das, S.; et al. Soil Moisture Model with Multi Angle and Multi Polarisation Risat-1 Data. *ISPRS Annals of the Photogrammetry, Remote Sensing and Spatial Information Sciences*, **2014**, *2, 145*.
32. Prevot, L.; Champion, I.; Guyot, G. Estimating surface soil moisture and leaf area index of a wheat canopy using a dual – frequency (C and X bands) scatterometer. *Remote Sens. Environ*., **1993**, 46, 331-339.
33. http://iopscience.iop.org/article/10.1088/1755-1315/105/1/012083/pdf